Human Movement Science 85 (2022) 102994

Contents lists available at ScienceDirect

Human Movement Science

journal homepage: www.elsevier.com/locate/humov

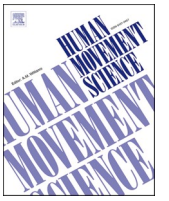

Hierarchical and synergistic organization of control variables during the multi-digit grasp of a free and an externally fixed object☆

Junkyung Song [a], Kitae Kim [c], Satyajit Ambike [b,**], Jaebum Park [a,d,e,*]

[a] Department of Physical Education, Seoul National University, Seoul, South Korea
[b] Department of Health and Kinesiology, Purdue University, West Lafayette, IN, USA
[c] Department of Sports Science, Korean Institute of Sports Science, Seoul, South Korea
[d] Institute of Sports Science, Seoul National University, Seoul, South Korea
[e] Advanced Institute of Convergence Science, Seoul National University, Seoul, South Korea

ARTICLE INFO

Keywords:
Multi-digit prehension
Referent aperture
Referent coordinate
Apparent stiffness
Grip stability
Equilibrium-point hypothesis

ABSTRACT

In the referent control theory, grip force emerges by designating the referent aperture (R_a) as a threshold position inside the object. This study quantified R_a and investigated whether the synergistic control of digit referent coordinate (*RC*) and apparent stiffness (k) depend on the external mechanical constraints on the hand-held object. Subjects held a motorized handle capable of adjusting the grip width and performed static multi-digit prehension tasks in which the handle was free and externally fixed in different conditions. The *RC* and k of individual digits were reconstructed from the changes in digit normal forces and the positions as the grip width was modulated. *RC*s of the thumb and virtual finger were used to calculate the width and midpoint of R_a, and synergy indices quantifying the task-specific covariation in the space of the digit normal forces and {*RC*, k} variables were computed. We found that the k and width of the R_a were larger when holding a free handle than the fixed handle. The higher stiffness in the free condition could be a strategy to ensure grip stability. The midpoint of R_a was skewed toward the virtual finger, reflecting different magnitudes of k for the two digits. Further, the normal forces and control variables {*RC*, k} displayed synergistic covariation for stabilization of the total grasping force. Finally, the synergies were weaker when the handle was externally fixed, demonstrating the dependence of synergies on external constraints. These results add to the current literature by demonstrating that grasp control involves modulation of digit apparent stiffness in addition to the referent coordinate and by identifying the synergistic organization of the control variables during static grasp.

1. Introduction

Grasping is a basic human behavior. Humans actively adjust mechanical and physiological variables to satisfy the constraints

☆ This manuscript is submitted to the special issue: "Understanding Movement Biomechanics: Tribute to Professor Vladimir M. Zatsiorsky".

* Correspondence to: J. Park, Seoul National University, 71-1, #414, 1 Gwanak-ro, Gwanak-gu, Seoul 08826, South Korea.
** Correspondence to: S. Ambike, Department of Health and Kinesiology, Purdue University, 800 W Stadium Ave., West Lafayette, IN 47907, USA.
E-mail addresses: sambike@purdue.edu (S. Ambike), parkpe95@snu.ac.kr (J. Park).

https://doi.org/10.1016/j.humov.2022.102994
Received 6 May 2022; Received in revised form 10 August 2022; Accepted 11 August 2022
Available online 17 August 2022

related to the movement of the object imposed by specific prehensile tasks. This process is governed in part by the central nervous system (CNS) that generates the neuronal command for the proper organization of the mechanical variables involved in the action. In the present work, we use the theory of referent configurations, based on the equilibrium point hypothesis (Feldman, 2015), to study the control of prehension.

According to the referent control theory, prehension via the opposition of the thumb and fingers is achieved by the specification of the referent aperture (R_a) (Ambike, Paclet, Zatsiorsky, & Latash, 2014; Feldman, 2015; Frenkel-Toledo, Yamanaka, Friedman, Feldman, & Levin, 2019; Latash, 2010; Latash, Friedman, Kim, Feldman, & Zatsiorsky, 2010; Pilon, De Serres, & Feldman, 2007). R_a is located inside the grasped object, and it is related to the referent positions of the digit tips – i.e., the position in space to which the current muscle activation attempts to drive the digit (Fig. 1A). Grip force at the digit-object interface arises because the object prevents the digits from approaching their corresponding referent positions (Pilon et al., 2007). In previous work, the midpoint of R_a was assumed to be located at the mid-point of the actual grip aperture during static prehension (Ambike et al., 2014; Latash et al., 2010), generating the equal and opposite digit forces necessary for a static grasp. However, the digit force is determined by the difference in the digit's actual and referent coordinates (RC) and the digit apparent stiffness (k) (Ambike, Mattos, Zatsiorsky, & Latash, 2016; Cuadra, Wojnicz, Kozinc, & Latash, 2020; Latash, 2020a, 2020b). Therefore, the assumption of the coincidence of the midpoints of R_a and the actual aperture for static grasping implicitly assumed equal apparent stiffnesses of the thumb and the opposing digits. There is some evidence supporting equal k for opposing digits during static prehension (Zatsiorsky, Gao, & Latash, 2006), however, this assumption has not been sufficiently tested. In particular, the apparent stiffness can be modulated by adjusting muscle co-contraction, and k is likely a control variable that could influence the stability of the grasp (Latash, 2018).

Therefore, the first goal of this study was to establish that the control of grasp involves modulation of the referent aperture as well as the apparent stiffness. We address this goal by comparing the grasp of a free object with the grasp of an externally constrained object, where grasp stability is ensured by the digits and by the structure of the object (i.e., fixed to the ground), respectively. Since the digit forces during prehension depend on external mechanical constraints (Park, Baum, Kim, Kim, & Shim, 2012; Park, Kim, & Shim, 2010), it is plausible that the control variables {RC, k}, are affected by the presence/absence of the external constraints as well. For example,

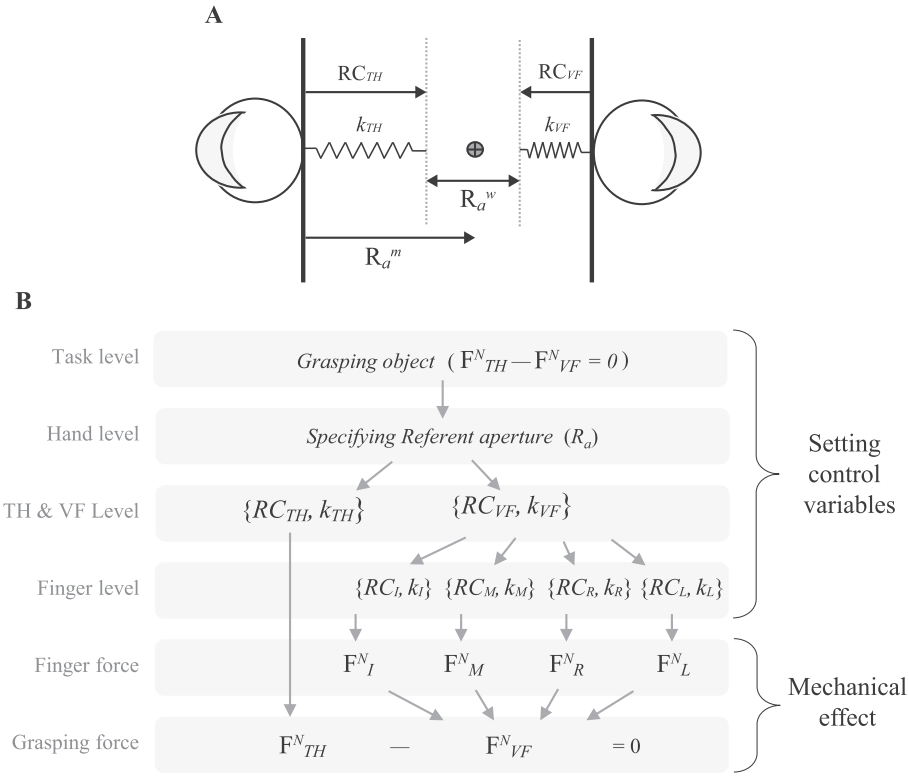

Fig. 1. (A) An illustration of the referent aperture (R_a) inside the grasped objects. The R_a is defined by referent coordinate (RC) of thumb (TH) and virtual finger (VF). Object prevents the digits from reaching the threshold position RC, and a normal force is generated depending upon the digit's apparent stiffness (k). R_a^w: width of referent aperture; R_a^m: midpoint of referent aperture. (B) A hypothetical scheme of neural control for grasping objects using five digits. R_a as a single control variable for producing grip force is specified at the hand level. At the thumb (TH) and virtual finger (VF) level, the R_a results in the RC and k of both digits. Specified {RC, k} in the virtual finger (VF) results in the pairs of {RC_i, k_i} for the individual fingers {i = index (I), middle (M), ring (R), and little (L) fingers} at the finger level. Individual normal finger forces (F_i^N) are generated by the corresponding pairs of the {RC, k}, and the grip force that satisfied the horizontal translation constraint (F_{TH}^N—$F_{VF}^N = 0$) is produced by the normal forces of the thumb (TH) and virtual finger (VF).

compared to the grip force on an object whose orientation is externally constrained, the grip force for the static prehension of a free object is higher. This increase is due to the higher forces of the lateral (index and little) fingers that assist in maintaining rotational stability of the free object (Park, Baum, et al., 2012). Since the higher grip force was aimed at improving stability, it is probable that the force changes were driven by a higher apparent stiffness. Therefore, we computed the R_a and {RC, k} of the digits during static prehension of a free and a constrained object, while ensuring that the magnitude of the grip force was same in both conditions. Our first hypothesis (H1) was that the apparent stiffness k for the digits will be higher when the digit forces are constrained and responsible for grasp stability, i.e., while grasping a free compared to an externally fixed object. Higher k will be accompanied by smaller RC for the digits so that the grip force is constant. The referent aperture arises from the digit RCs (cf. Fig. 1A), and this would lead to a larger referent aperture while grasping the free object. In addition, our second hypothesis (H2) was that the midpoint of R_a would not be located at the center of the actual aperture, reflecting that k for the thumb and the four fingers (combined) are different.

The second goal of this study was to quantify the synergistic covariation between these control variables during the two types of static prehension. Various mechanical, physiological and control variables involved in motor control are organized in a hierarchy with redundancy at all levels. The multi-digit prehension has been viewed as two-levels of hierarchy, including the thumb and virtual finger as an upper-level and the individual fingers as a lower-level (Gao, Latash, & Zatsiorsky, 2004). The hierarchical organization for multi-digit prehension within the referent control theory is presented in Fig. 1B, which is an expansion of the scheme of four finger pressing task (Reschechtko & Latash, 2018). The controller designates R_a at the task level, and this leads to defining {RC, k} for the higher-level effectors (i.e., the thumb and the virtual finger (Arbib, Iberall, & Lyons, 1985; MacKenzie & Iberall, 1994) — a virtual digit that has the same mechanical effect on the object as the four fingers combined). Since the virtual finger is composed from four fingers, the specified RC and k of the virtual finger arises from {RC, k} variables for the individual fingers. Since the number of input variables (at a given level of the hierarchy, called the upper level) is smaller than the number of the output variables (at the adjacent lower level in the hierarchy), there are few-to-many maps linking each pair of consecutive levels of the hierarchy, reflecting the redundancy in the system. This redundancy is exploited by the central controller: the upper-level variables are stabilized by covaried adjustment within

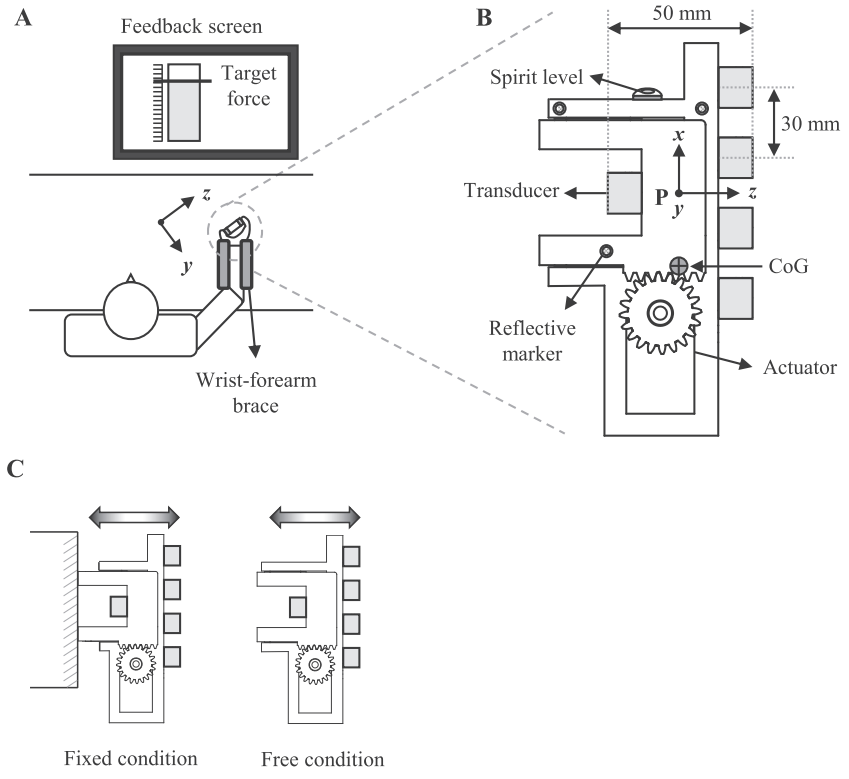

Fig. 2. Experimental setup. (A) Subjects' forearm and wrist were held securely on a rigid brace in a natural grasping hand position. A monitor located at eye level approximately 1 m away from the subjects was used for visual feedback of digit normal forces. Note that the visual force feedback was provided only in the fixed prehension condition. (B) Description of the motorized handle. A handle-fixed coordinate frame was located at point P. The distance between the centers of adjacent transducers on the fingers side was 30 mm, and the transducer corresponding to the thumb was located in the center of the middle and ring finger transducers along the x-axis. Grip width was 50 mm along the z-axis. A servo actuator (Dynamixel MX-64 T Robot servos, ROBOTIS, South Korea) was mounted on the frame of the handle to make capable of position and velocity control, and both parts of the handle were connected by two linear guides, allowing the changes of grip width to expand (i.e., moving outward) and contract (i.e., moving inward). A small spirit level and reflective markers were attached to the handle frame. (C) The handle was designed to fix one side of the frame to an immovable steel frame on the table. It made possible fixed-object prehension (Fixed) without mechanical constraints as well as free object prehension (Free).

the redundant set of lower-level variables. Such task-specific covariation is quantified using synergy analysis (Ambike et al., 2016). This scheme was verified for manual behaviors when covariation among the control variables of each finger stabilized upper-level variables in a four-finger pressing task (Reschechtko & Latash, 2018). For grasping, however, only stabilization of *mechanical variables* (digit forces and moments) at different levels in the control hierarchy has been reported (Gorniak, Zatsiorsky, & Latash, 2009; Park, Han, & Shim, 2015; Shim, Latash, & Zatsiorsky, 2003, 2005a; Zatsiorsky, Gregory, & Latash, 2002b; Zatsiorsky & Latash, 2008); no attempt has been made to examine the stabilization of *control variables* in the hierarchy. Therefore, our third hypothesis (H3) was that the control variables in the few-to-many maps presented in Fig. 1B, including {*RC*, *k*} and the digit forces, would display synergistic organization. Furthermore, we expected that the synergies in the {*RC*, *k*} variables and in the digit forces, quantified at the same level, would be correlated since both synergies quantify the same behavior. Finally, our fourth hypothesis (H4) was that the strength of covariation between the variables would be larger during free object prehension compared to fixed object prehension, especially at the higher level of the hierarchy due to the aforementioned external factors. To test these hypotheses, we constructed a motorized handle that changed the grip width and allowed us to estimate *RC* and *k* during static prehension.

2. Methods

2.1. Subjects

Ten healthy young subjects (8 males and 2 females), age 29.9 ± 3.87 (mean ± SD) years, mass 71.9 ± 6.06 kg, and height 1.72 ± 3.33 m, voluntarily participated in the current experiment. The hand dominance of the subjects was determined using the Edinburgh handedness inventory (Oldfield, 1971), and all subjects were right-handed. They had no history of neurological or musculoskeletal disorder that could affect the completion of the experimental tasks (by self-report). All participants gave informed consent in accordance with the recommendations of the Seoul National University Institutional Review Board (IRB No. 2007/0 02–023).

2.2. Apparatus

We constructed a motorized handle (Fig. 2B) that was capable of adjusting the grip width at constant speed. Individual digit forces were measured using five six-component force/torque transducers (Nano-17, ATI Industrial Automation, Garner, NC, USA), which were attached to the motorized-handle (Fig. 2B). The transducers were aligned in the *x*-*z* plane of the local coordinate system of the handle. 100-grit sandpapers were attached on the contact surfaces of the transducers to provide sufficient friction (Savescu, Latash, & Zatsiorsky, 2008). Also, we confirmed that the position of center of gravity (CoG) of the handle-sensor assembly was along the *z*-axis close to the middle of the grip width (Fig. 2B). The mass of the handle with transducers was 0.57 kg. All force signals were set to zero before each trial began and sampled at 200 Hz and digitized with an analog-to-digital converter (Gen5, AMTI, Watertown, MA, USA).

Three light-weight spherical reflective markers (4 mm in diameter) were secured to the handle for the measurement of the handle orientation and the horizontal displacement caused by the embedded motor (Fig. 2B). The marker positions were recorded at 200 Hz using a motion capture system (OptiTrack, Natural Point Inc., Corvallis, OR, USA). The motion and finger force measurement systems were synchronized. A 24-in. monitor, placed at 0.8 m in front of the subject, provided real-time visual feedback of force (Fig. 2A). A customized LabVIEW program (National Instruments) was used for acquiring the force data, controlling the motorized handle, and providing real-time visual feedback.

2.3. Experimental procedure

The subjects sat in a chair, and positioned their right arm as follows: the right forearm and wrist were placed in a rigid forearm brace above the table with their shoulder at approximately 45° abduction and 30° flexion, and the elbow at 60° flexion (Fig. 2A). In particular, the forearm and wrist were strapped to the arm brace at the neutral position; thus, the motions of flexion-extension and radial-ulnar deviation of the wrist joint were minimized. The main experimental task was to hold the motorized handle with the right hand in two conditions: Free and Fixed. For the Free condition, the digits were responsible for maintaining the translational and rotational equilibrium of the handle. In contrast, the handle was firmly fixed to the table in the Fixed condition (Fig. 2C), so that the digit forces were neither responsible for nor were they able to influence the equilibrium of the handle.

The subjects were instructed to hold the handle with five digits in the grasping plane shown in Fig. 2A. For the Free condition, the magnitudes of grip force were not prescribed, and visual grip force feedback was not provided. We instructed the subjects to hold the handle comfortably using "natural" grip force and orient the handle vertically via the spirit level before the onset of the trial. We also instructed the subjects not to make any intentional change in the orientation of the handle when the grip aperture was modulated. The measurement started when the subjects reported a "*ready*" sign and the experimenter confirmed the vertical orientation of the handle. Each trial lasted 15 s. For the first 5 s, the subjects held the handle stationary without any aperture adjustment. At a random time between 5 and 8 s after trial onset, the width of the handle expanded by 20 mm, and then contracted to the initial width at a rate of 20 mm/s (Ambike et al., 2016; Reschechtko & Latash, 2017, 2018). Thus, the initial 50 mm grip width expanded to 70 mm and then returned to its initial value. The subjects were given the following instructions: "*do not react to the movements of handle*", and "*do not adjust your commands to the hand*" and "*continue holding the handle until the end of the trial*" (Feldman, 1966; Latash, 1994).

For the Fixed condition, the thumb side of the handle was firmly fixed to the table (Fig. 2C), and the coordinate frame of the fixed handle was aligned with the table-fixed coordinate frame. With this arrangement, the table ensured the static equilibrium of the handle, but the motor was still able to vary the grip aperture. We instructed the subjects to hold the (fixed) handle naturally as if they

were grasping a free object. The subjects received visual feedback on the grip force (i.e., the normal force of the thumb; Fig. 2A), and the target force was equal to the subject's average normal thumb force over 50 ms of steady state grasping before the handle movement in the FREE condition. This process equalized the average effort of the digits between the two experimental conditions. The measurement started when the subject's grip force matched the prescribed value. Providing real-time visual force feedback when the grip width changed could interfere with the instruction not to voluntarily intervene; therefore, the visual feedback was removed 5 s after trial onset, and the subjects were instructed to hold the handle with the same effort until the end of the trial. Like the FREE condition, the grip width adjustment was initiated at a random time between 5 and 8 s from the onset of the trial.

The FREE and FIXED experimental conditions were conducted over three days. The first day was for familiarizing the subject to the experimental setup and tasks; no data were collected. The second and third day were for the data collection in FREE and FIXED condition, respectively. The subjects performed 30 trials in each condition per day and had a mandatory 45 s rest after the completion of each trial. Also, subjects were required to ask for additional rest if they felt fatigue. None of the subject reported any fatigue. The total duration of the experiment per day was ~60 min.

2.4. Data analysis

Force and position data were low-pass filtered with a fourth-order, zero-lag Butterworth filter with a cutoff of 10 Hz (Ambike, Zhou, Zatsiorsky, & Latash, 2015). We restricted the analysis to the *x*-*z* grasping plane (Zatsiorsky, Gregory, & Latash, 2002a), which was coincided with the frontal plane of the handle reference (Fig. 2B). Therefore, the analysis of digit force data for determination of control variables was limited to the normal forces along the *z*-axis. Similarly, we used marker position data along the z-axis of the table-fixed coordinate frame, which was parallel to the direction of aperture adjustment. Since the motorized handle was not fixed in the FREE condition, the handle- and table-fixed *z*-axes may get misaligned. Hence, the position data in the FREE condition were visually inspected to ensure that the *z*-axes of the two frames were aligned during static prehension and aperture adjustment; we rejected trials in which the alignment between the two *z*-axes was more than ±3°. We also visually inspected the force profiles and rejected trials where we observed significant force drift over time, mismatch in the prescribed and produced force by more than ±5% at the steady-state force production phase (for the FIXED condition), and abrupt changes in force during the handle expansion phase. The average percentage of accepted trials across the subjects was 92%.

The force and position data for the multiple trials were aligned with respect to t_0 – the onset of the motor on the handle (Fig. 3A). We defined analysis phases as follows: (1) static prehension phase for 50 ms before t_0 and (2) the handle expansion phase until the peak digit forces were observed. We confirmed that peak digit forces occurred at the instant of maximum handle expansion. All dependent variables were analyzed at two levels of the control hierarchy: the upper level created by the thumb (TH) and virtual finger (VF), and the lower level created by the four fingers (i.e., index, I; middle, M; ring, R; little finger, L).

2.4.1. Mechanical constraints of the task

For static prehension in the 2D plane, the following constraints must be satisfied in the FREE condition: 1) The sum of the normal forces of the four fingers must equal the normal force of the TH to satisfy the horizontal translation constraint. 2) The sum of the tangential forces produced by all five digits must equal the weight of the grasped object. 3) The resultant moment produced by all five-digit forces must be zero since no external torque acted on the handle. For the FIXED condition, there was no need to satisfy these constraints to maintain static equilibrium.

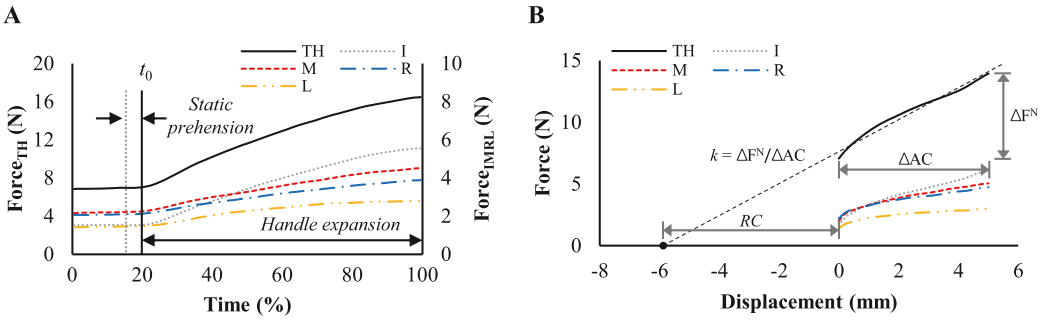

Fig. 3. (A) Representative time-series data of each digit normal forces during static prehension and handle expansion phases. The time is normalized to 100% from the trial onset to when the motorized handle is maximally widened. The scale of the left vertical axis reflects the thumb (TH) force level, and the right axis refers to the force of individual finger {index (I), middle (M), ring (R), and little (L) fingers}. The vertical solid line indicates the time of the onset of the actuator (t_0). The dashed vertical line represents the time point before 50 ms of the driving actuator. (B) Example of sensor displacement versus digit normal force data in handle expansion phase. The net change in the normal force (ΔF^N) and digit displacement (ΔAC) of each digit were calculated. The ΔF^N and ΔAC were obtained by subtracting the initial value from its final value. The initial values were obtained from the average normal force and corresponding digit position in the static prehension phase, and the final values were computed as the average values during the final 10 ms of handle expansion phase. k of each digit was computed according to Hooke's law, $k = \Delta F^N/\Delta AC$, in unit of N/mm. The *RC* (in unit of mm) of each digit was computed as $RC = F^N/k$ with the initial digit-tip position (i.e., AC in Eq. 3) was defined as zero. Thus, the calculated *RC* represented the threshold position where the digit normal forces were stationary prior to the handle expansion.

2.4.2. Reconstruction of RC and k at two hierarchical levels

Our purpose was to quantify the referent aperture, specifically, the width (R_a^w) and midpoint (R_a^m) of R_a. These quantities depend on the *RC* and *k* of TH and VF. Therefore, we computed the *RC* and *k* values for each digit separately using the methods of Reschechtko and Latash (2018). We modeled the normal force of digit *i* along the *z*-axis (F_i^N) as:

$$F_i^N = k_i \times (AC_i - RC_i), \tag{1}$$

where AC_i is the actual coordinate of the digit-tip along the *z*-axis. We assumed a linear relation between the force and the difference in the actual and referent coordinate (see the representative force-displacement profiles for the digits in Fig. 3B). To validate this assumption, we regressed separately the normal force against the *z*-axis displacement of each digit. We accepted trials in which the *R* values of the regressions for all the digits were above 0.9 (Reschechtko & Latash, 2017). The across-subject average for the accepted trials was 24.2 out of 30 repetitions.

The details of the computation of *RC* and *k* are described in Fig. 3B. To generate a grasping force, the *RC* of both TH and VF must lie inside the object (Fig. 1A). Note that the sign of RC will depend on the location and orientation of the coordinate frame used for the computation; similarly, the normal force of the TH and VF, when expressed in the same handle-fixed coordinate frame, will be of opposite signs. For further analysis, we used the absolute values of all normal forces, and we expressed *RC*s as positive distances from the actual location of the corresponding digit before the grip width was modulated, as shown in Fig. 1A. We obtained pairs of digits {*RC*, *k*} for all selected trials. Using the *RC* of TH and VF, we computed width and midpoint of R_a (i.e., R_a^w and R_a^m, respectively) as follows:

$$R_a^w = grip\ width - |RC|^{TH} - |RC|^{VF}, \tag{2}$$

$$R_a^m = |RC|^{TH} + \frac{R_a^w}{2} = 0.5 \times \left[grip\ width + |RC|^{TH} - |RC|^{VF} \right], \tag{3}$$

where grip width was 50 mm, and R_a^m was determined from the initial TH position before the grip width changed.

2.4.3. Permutation analysis of RC and k

We investigated whether the control variables within the referent configuration hypothesis, {*RC*, *k*}, which are called elemental variables (EVs) within the synergy literature, displayed covariation to stabilize task-specific performance variables (PVs). This analysis was conducted separately for Free and Fixed conditions and for the upper and lower level of the control hierarchy. For the upper level, the total normal force F_{TOT}^N can be expressed as

$$F_{TOT}^N = |RC|_{TH} \times k_{TH} - |RC|_{VF} \times k_{VF}. \tag{4}$$

Eq. 4 indicates that the control variables for TH and VF are constrained to produce zero total force, so that the handle remains static. For the lower level, the VF normal force (F_{VF}^N) arises from the {*RC*, *k*} for the fingers:

$$F_{VF}^N = \sum_i RC_i \times k_i. \tag{5}$$

We quantified the synergy in which {*RC*, *k*} of the TH and VF covary in a 4-dimensional space to stabilize F_{TOT}^N at the upper level. At the lower level, we quantified the {*RC*, *k*} synergy in the 8-dimensional space that stabilizes F_{VF}^N. Finally, we also quantified the synergy in the corresponding 2-dimensional {*RC*, *k*} space stabilizing the normal force for the TH and the VF at the upper level, and for the four fingers (I, M, R, L) at the lower level. For digit *i*, the EVs and PVs are related simply as: $F_i^N = RC_i \times k_i$. This constraint on the EVs is hyperbolic, and the constraints expressed in Eqs. 4 and 5 are sums of hyperbolas. These constraints are highly non-linear and linearizing these systems for the synergy analyses is questionable. Therefore, we utilized permutation analysis to identify task-specific covariation in the EVs (Muller & Sternad, 2003). We generated surrogate PVs using the respective constraint equations for each analysis after random permutations of the EVs. The permutation operation removes the task-specific covariation in the EVs; if the variability in the corresponding surrogate PVs is higher than the original PV set, we conclude that the EVs contained task-specific covariation. We computed the standard deviation (SD) of the surrogate and actual PV data, and the ratio of SD (R^{SD}) of the surrogate and actual PV data was a quantity of the synergy index within the {*RC*, *k*} space. This analysis was conducted separately for both hierarchies and individual digits. Detailed computation procedures for R^{SD} can be found in Reschechtko and Latash (2018). Theoretically, if R^{SD} is >1, it means that the *RC* and *k* within original data covaried to stabilize the outcome digit force. However, we applied the more conservative criterion $R^{SD} > 2$ to infer task-specific covariation (Reschechtko & Latash, 2018).

2.4.4. UCM-based analysis of variance on referent aperture and digit normal forces

The uncontrolled manifold (UCM) approach was employed to analyze the digit F^N at the two hierarchical levels (Park et al., 2015). For the upper level, the TH and VF normal forces were the EVs, the total normal force was the PV. The TH and VF normal force magnitudes must covary positively so that their difference is stabilized around zero, and the object remains static. Therefore, the EVs and the PV are related by the constraint: $F_{TOT}^N = F_{TH}^N - F_{VF}^N$. The Jacobian relating small changes in the EVs to changes in the PV was [1,−1]. For the lower-level analysis, the individual finger forces were the EVs, the VF normal force was the PV, related by the constraint: $F_{VF}^N = \sum F_i^N$, for i = {I, M, R, L}, and the corresponding Jacobian was [1,1,1,1]. For both analyses, the null space of the corresponding Jacobian defines the uncontrolled manifold (UCM). Changes in the EVs along the UCM do not change the PV; however,

changes in the EVs orthogonal to the UCM change the PVs.

For each of these analyses, the across-trial EV data was decomposed into two variance components: one along the corresponding UCM (V_{UCM}), and another orthogonal to the UCM (V_{ORT}). The synergy index (ΔV) was then calculated using the normalized difference in V_{UCM} and V_{ORT}. The ΔVs were log-transformed using the Fischer transformation to account for the bounds on the synergy index (Park, Lewis, Huang, & Latash, 2013; Wu, Zatsiorsky, & Latash, 2012).

2.5. Statistics

Our first and second hypotheses were related to the quantification of {*RC, k*} of individual digits and the midpoint of R_a in the Free and Fixed conditions. To test the first hypothesis (H1), we performed separate *Digit* × *Type* repeated-measures (RM) ANOVAs on *RC* and *k*. This analysis was performed separately at each hierarchical level. The factor *Digit* had two levels (TH and VF) for the upper-level analysis and four levels (I, M, R, L) at the lower-level analysis. The factor *Type* had two levels (Free and Fixed) for both analyses. Also, we performed separate paired *t*-tests on R_a^w and R_a^m to determine the effect of *Type* on the referent aperture. To test the second hypothesis (H2), we performed separately for the Free and Fixed conditions single-sample *t*-tests to compare the computed midpoint of the referent aperture (R_a^m) with the value of 25 mm – the midpoint of the actual aperture. The third and fourth hypotheses were about the quantification of the synergies within the control variables and comparison between two prehension conditions. To test the third hypothesis (H3), all the R^{SD} values, quantifying synergistic organization of the control variables, were compared with the critical value of 2 using separate single-sample *t*-tests for all digits in both conditions. Similarly, ΔV_Z values were compared with the relevant critical values using single-sample *t*-tests. The critical value of ΔV_Z was 0 for the upper-level F^N analyses and 0.55 for the lower-level F^N analysis since the bounds on the synergy indices were different depending on the nullity of the Jacobian. Also, the correlation analyses between R^{SD} and ΔV_Z for total normal force stabilization was performed separately in the Free and Fixed conditions. Finally, to test the fourth hypothesis, synergies within space of {*RC*, *k*} were analyzed using RM ANOVAs with factors *Hierarchy* (two levels: upper and lower level) and *Type*. Similarly, the F^N-stabilizing ΔV_Z (and corresponding V_{UCM} and V_{ORT}) were tested using the same RM ANOVA.

Mauchly's sphericity test was used to confirm the assumptions of sphericity, and their violations were corrected by the Greenhouse-Geisser estimation. All pairwise comparisons with Bonferroni corrections were performed to explore significant interaction effects, or significant main effects when no interaction was observed. The effect size was quantified using partial eta-squared (ηp^2) for the ANOVAs and Cohen's *d* for the *t*-tests. We conducted all statistical analyses using SPSS 24.0 (IBM, Armonk, NY), and the level of significance was set at $p < 0.05$.

The current experiment measured both normal and tangential digit forces; both groups of forces are essential to ensure a stable static grasp. However, we restricted our analyses to the normal forces. Our results and interpretations would be problematic if there was interaction between the normal and tangential forces. Therefore, we tested the independence of the normal and tangential forces via principal component analysis (PCA) with variance maximizing rotation to observe the configuration of digit normal (F^N) and tangential (F^T) forces. This analysis was conducted using four components of digit forces (F^N_{TH}, F^N_{VF}, F^T_{TH}, F^T_{VF}) over repeated trials for each subject and condition (Free and Fixed) separately. The Kaiser Criterion (i.e., extracted PCs should be the eigenvectors with eigenvalues >1) was employed to define the significant PCs and loading coefficients (Kaiser, 1960).

3. Results

To determine task performance, we calculated the orientation (angle) of the handle (θ_{Handle}) with respect to the horizontal axis in the *x*-*z* plane in the Free condition. The results showed that the θ_{Handle} was not changed, but maintained at zero level over the time. This was confirmed by Bayesian single-sample *t*-test with Jeffrey-Zellner-Siow prior performing to compare the θ_{Handle} to zero. Thus, it seems that the participants were able to maintain the orientation of the handle as instructed sufficiently.

Recall that the analyses of the forces and referent variables is conducted for the normal (*z*) direction, independent of the tangential forces produced by the digits. The PCA with four components of digit forces (F^N_{TH}, F^N_{VF}, F^T_{TH}, F^T_{VF}) showed that the first two significant PCs explained >99.26 ± 0.27% and 69.85 ± 2.64% of the variance for the Free and the Fixed conditions, respectively. Average loadings across subject for the Free and Fixed conditions are listed in Table 1, and the significant loadings (> 0.5) are shown in bold. The normal forces of the TH and VF had large loadings in the PC1, whereas the two tangential force components grouped into PC2. This grouping pattern appeared similarly in the Free as well as in the Fixed condition. These results suggest the independence of the normal and the tangential digit forces during our tasks.

Table 1
Loadings of principal components (PC1 and PC2) of digits normal and tangential finger forces in free (Free) and fixed object (Fixed) conditions.

	Free		Fixed	
	PC1	PC2	PC1	PC2
F^N_{TH}	**0.980 (0.005)**	0.162 (0.028)	**0.769 (0.035)**	0.067 (0.087)
F^N_{VF}	**0.978 (0.005)**	0.175 (0.028)	**0.793 (0.037)**	0.116 (0.053)
F^T_{TH}	0.118 (0.053)	**0.975 (0.005)**	−0.068 (0.069)	**0.654 (0.164)**
F^T_{VF}	−0.079 (0.054)	**−0.975 (0.004)**	0.006 (0.049)	**−0.645 (0.169)**

Averaged loading factors across subjects. The values in parentheses indicate standard errors. Significant loadings (> |0.5|) are shown in bold. F^N_{TH}: thumb normal force; F^N_{VF}: virtual finger normal force; F^T_{TH}: thumb tangential force; F^T_{VH}: virtual finger tangential force.

3.1. Values of control variables, RC & k

The upper-level *RC* for TH in both conditions was significantly larger than the VF *RC*, and the *RC* in the Fixed Condition was significantly higher than that of the Free Condition (Fig. 4B). In contrast, *k* was significantly larger for the VF than TH, and *k* of TH and VF was larger in the Free condition (Fig. 4C). These results were supported by significant main effects of *Digit* (*RC*: $F_{[1,9]} = 87.15$, $p < 0.001$, $\eta p^2 = 0.91$; *k*: $F_{[1,9]} = 25.15$, $p = 0.001$, $\eta p^2 = 0.74$) and *Type* (*RC*: $F_{[1,9]} = 21.40$, $p = 0.001$, $\eta p^2 = 0.70$; *k*: $F_{[1,9]} = 16.98$, $p = 0.003$, $\eta p^2 = 0.65$) in the ANOVAs.

The across-finger changes in *RC* and *k* were dissimilar in the Free and Fixed tasks. This was reflected in significant *Digit* × *Type* interactions for both variables (*RC*: $F_{[3,27]} = 6.02$, $p = 0.003$, $\eta p^2 = 0.40$; *k*: $F_{[3,27]} = 9.49$, $p < 0.001$, $\eta p^2 = 0.51$). The post-hoc comparisons revealed that in the Free condition, the *RC* for the index finger was lower than that for the other three fingers, and the opposite pattern appeared for the *k* ($p < 0.05$). In the Fixed condition, the *RC* was R > L, and the *k* was I > M and R ($p < 0.05$). Further, the *RC* of the I and M was significantly lower in the Free than the Fixed condition, whereas the *k* of that fingers in the Free was significantly larger than the Fixed condition ($p < 0.05$).

The width of referent aperture (R_a^w) in the Free and Fixed condition were 29.17 ± 1.43 and 16.79 ± 3.07 mm, respectively (Fig. 5); the paired *t*-test found that R_a^w was significantly larger in the Free condition ($t_{[9]} = 4.63$, $p = 0.001$, Cohen's $d = 1.46$). The midpoint of referent aperture (R_a^m) was significantly skewed toward VF from the center of the actual aperture (Fig. 5). The average R_a^m was 28.24 ± 1.77 mm from the TH in the Free condition, and 29.14 ± 0.69 mm in the Fixed condition. These unbalanced locations of R_a^m were confirmed by the single-sample *t*-tests, which showed that the R_a^m were significantly larger than the value of 25 (i.e., midpoint of the grip width) (Free: $t_{[9]} = 5.79$, $p < 0.001$, Cohen's $d = 1.83$; Fixed: $t_{[9]} = 5.99$, $p < 0.001$, Cohen's $d = 1.89$).

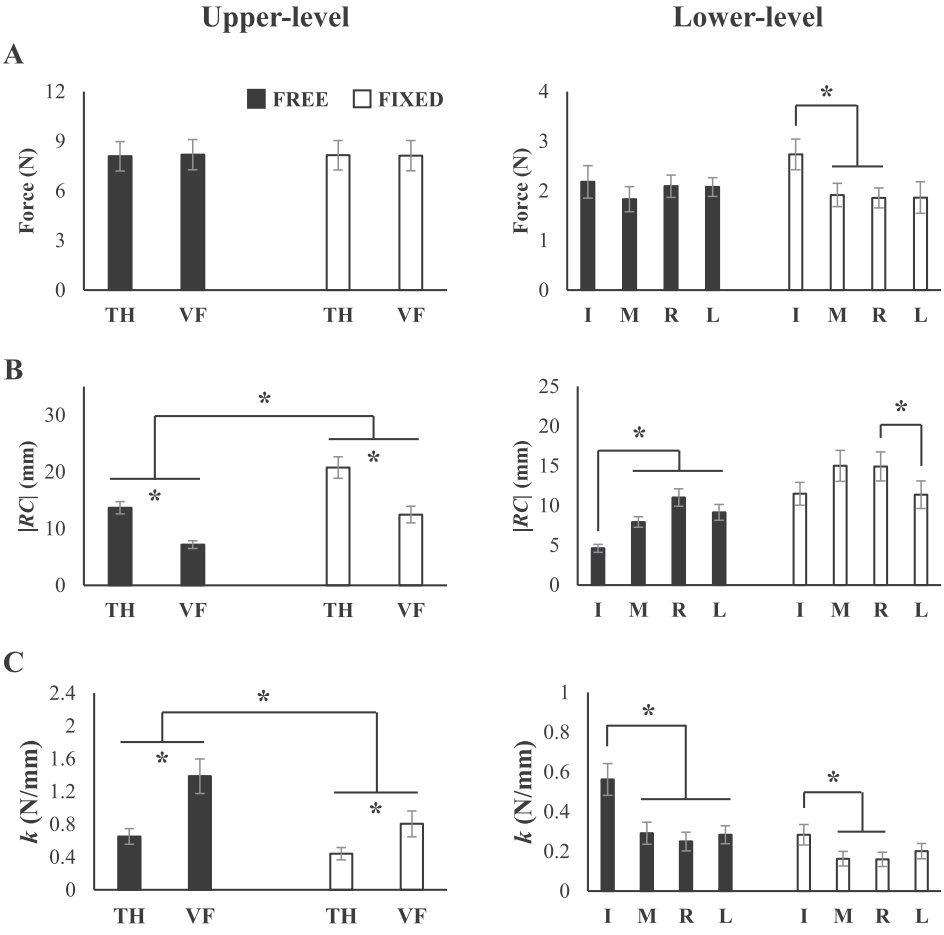

Fig. 4. Across-subject mean and standard errors of (A) digit normal forces, (B) *RC*, and (C) *k* for the upper and lower hierarchies. The upper level (left panel) includes the thumb (TH) and virtual finger (VF), and the lower level (right panel) contains the index (I), middle (M), ring (R), and little (L) finger. The solid bars and the open bars indicate the Free and Fixed, respectively. The asterisks indicate the presence of statistical differences between digits and conditions.

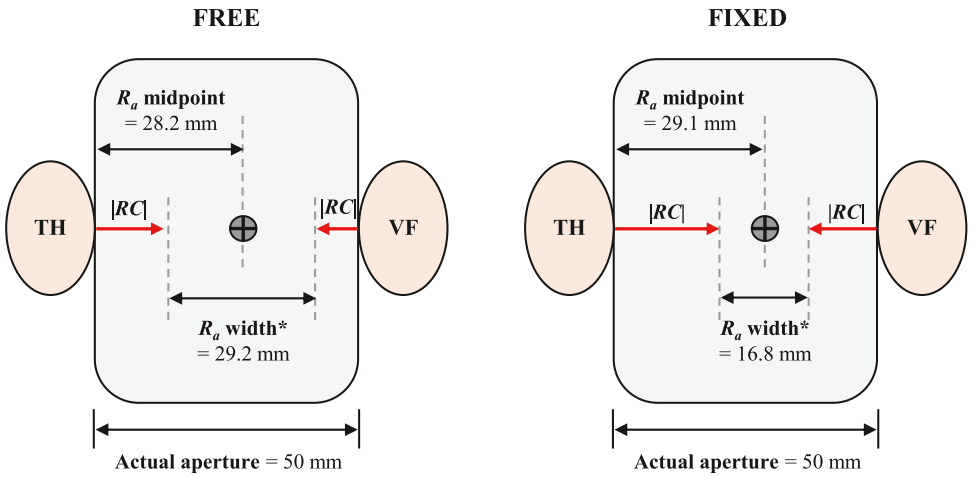

Fig. 5. An illustration for width (R_a^w) and midpoint (R_a^m) of referent aperture obtained in FREE (left) and FIXED (right). The R_a is determined by magnitudes of the *RC* of the thumb (TH) and virtual finger (VF). The grey circle inside the rectangular object is the location of R_a^m, which is skewed toward the virtual finger (VF).

3.2. Permutation-based analyses to quantify synergies in {RC, k} spaces

Single sample *t*-test for comparing R^{SD} with the critical value of 2 revealed {*RC*, *k*} synergies in all cases except for the lower-level FREE condition (upper-level FREE: $t_{[9]} = 23.60$, $p < 0.001$, Cohen's $d = 7.46$; upper-level FIXED: $t_{[9]} = 5.25$, $p = 0.001$, Cohen's $d = 1.66$; lower-level FIXED: $t_{[9]} = 5.69$, $p < 0.001$, Cohen's $d = 1.79$). The upper-level R^{SD} values, which quantified the covariation in the 4-dimensional {*RC*, *k*} space of the TH and VF for stabilizing F_{TOT}^N, were significantly larger in the FREE than the FIXED condition (Fig. 6). In contrast, the lower-level R^{SD} quantifying synergies within the 8-dimensional space of {RC_i, k_i} was smaller in the FREE condition. These findings were confirmed by *Hierarchy* × *Type* RM ANOVA, which showed significant interaction ($F_{[1,9]} = 667.93$, $p < 0.001$, $\eta p^2 = 0.99$).

We further quantified {*RC*, *k*} synergies for the individual digits. The across-trial *RC* and *k* data for individual digits and conditions pooled across subjects and the across-subject average of the R^{SD} values are presented in Fig. 7. The single-sample *t*-tests showed significant synergies within the {*RC*, *k*} space in all digits except the middle finger in the FREE condition (Fig. 7A; TH: $t_{[9]} = 3.64$, $p = 0.005$, Cohen's $d = 1.15$; VF: $t_{[9]} = 6.94$, $p < 0.001$, Cohen's $d = 2.19$; I: $t_{[9]} = 2.37$, $p = 0.042$, Cohen's $d = 0.74$; R: $t_{[9]} = 2.81$, $p = 0.021$, Cohen's $d = 0.88$; L: $t_{[9]} = 3.86$, $p = 0.004$, Cohen's $d = 1.22$). For the FIXED condition, however, there were synergies only in the upper-level digits (Fig. 7B; TH: $t_{[9]} = 7.17$, $p < 0.001$, Cohen's $d = 2.26$; VF: $t_{[9]} = 4.68$, $p = 0.001$, Cohen's $d = 1.47$).

The individual digit R^{SD} were different between control hierarchy depending on the FREE and FIXED conditions. For the upper level, the R^{SD} was larger in the FIXED than in FREE condition for both TH and VF. In contrast, the R^{SD} of the four fingers (i.e., lower-level I, M, R, and L) were larger in the FREE than in FIXED condition. These results were supported by *Digit* × *Type* RM ANOVA performed separately for each hierarchy. Both analyses showed significant main effect of *Type* (upper-level: $F_{[1,9]} = 10.74$, $p = 0.01$, $\eta p^2 = 0.54$; lower-level: $F_{[1,9]} = 6.36$, $p = 0.03$, $\eta p^2 = 0.41$).

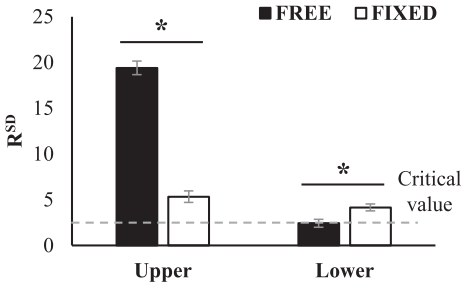

Fig. 6. Across-subject mean and standard errors of R^{SD} for each hierarchy and prehension condition. The upper level R^{SD} are determined using the 4-dimensional {RC_i, k_i} values (i = thumb, TH, and virtual finger, VF), and the lower level using 8-dimensional {RC_i, k_i} (i = index (I), middle (M), ring (R), and little (L) finger). The solid bars and open bars indicate the FREE and FIXED, respectively. The dashed line represents the critical R^{SD} value. The asterisks indicate significant differences between prehension conditions.

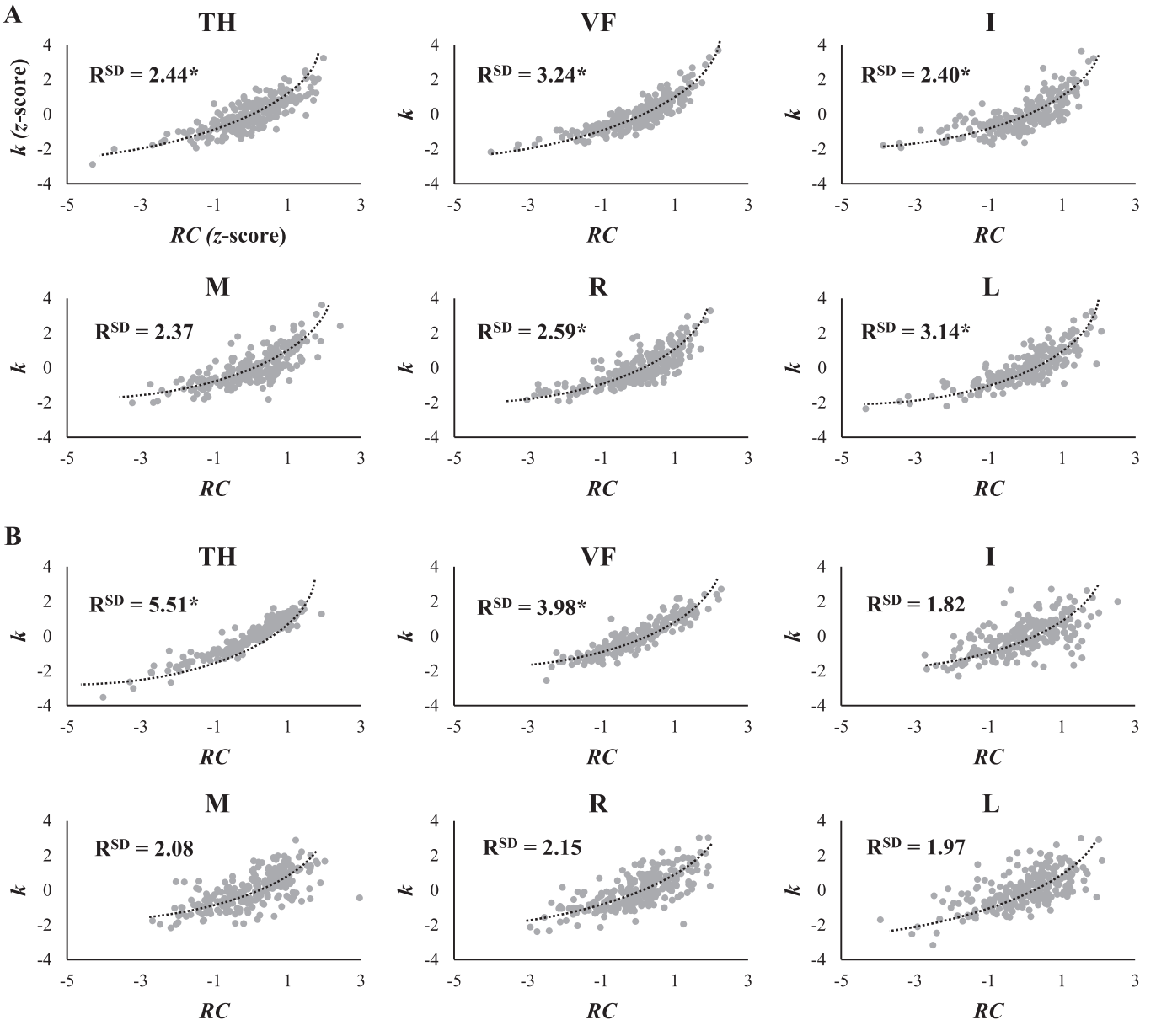

Fig. 7. The scatter plots of *RC* and *k* for individual digit in the (A) Free and (B) Fixed conditions. Originally, the *RC* and *k* were calculated in units of mm and N/mm, respectively. In figure, the {*RC*, *k*} pairs of each digit were normalized to z-scores to pool across trials and subjects. Average R^{SD} for across subjects is presented with hyperbola regression line for each digit. TH: thumb; VF: virtual finger; I: index; M: middle; R: ring; L: little fingers.

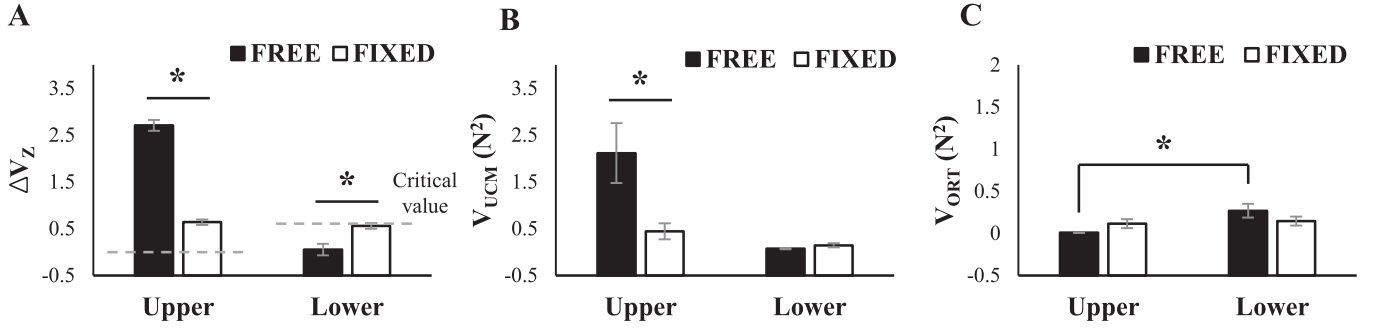

Fig. 8. (A) Across-subject mean and standard errors of synergy indices (ΔV_Z) stabilizing upper and lower-level digit normal forces in the Free and Fixed condition. (B) and (C) show variance in the space of the uncontrolled manifold (V_{UCM}) and orthogonal to the V_{UCM} (V_{ORT}), respectively. The solid and open bars indicate the Free and Fixed, respectively. Horizontal dashed lines represent critical ΔV_Z values (= 0 for upper-level, and ≈ 0.55 for lower-level). The asterisks indicate significant differences between condition and hierarchy.

3.3. UCM-based synergy indices of digit forces

The synergy indices for the stabilization of net grip force were higher than the critical value only at the upper level (FREE: $t_{[9]} = 22.88$, $p < 0.001$, Cohen's $d = 7.23$; FIXED: $t_{[9]} = 10.99$, $p < 0.001$, Cohen's $d = 3.47$). In particular, ΔV_Z stabilizing F^N_{TOT} at the upper level was greater in the FREE than in the FIXED condition (Fig. 8A). In contrast, at the lower level, the finger normal forces that yield F^N_{VF} showed the opposite pattern (Fig. 8A). This was supported by a *Type* × *Hierarchy* interaction ($F_{[1,9]} = 119.93$, $p < 0.001$, $\eta p^2 = 0.93$). The V_{UCM} for the FREE condition was greater than FIXED condition at the upper-level, and there was no significant difference at the lower-level (Fig. 8B). Significant difference in V_{UCM} between hierarchy was observed only in the FREE condition. In the case of V_{ORT}, there were no significant differences of two levels of Type in both hierarchies, and in the FREE condition, the lower-level was significantly larger than the upper-level (Fig. 8C). These finding were confirmed by significant *Type* × *Hierarchy* interactions (V_{UCM}: $F_{[1,9]} = 10.65$, $p = 0.01$, $\eta p^2 = 0.54$; V_{ORT}: $F_{[1,9]} = 7.42$, $p = 0.023$, $\eta p^2 = 0.45$).

3.4. Relationship between the synergy indices obtained from the permutation and UCM analyses

The R^{SD} values (obtained from permutation analysis) were compatible with the ΔV_Z values (obtained from UCM analysis). For the regression analysis, the pooled data across all subjects were used separately for the two conditions and hierarchies (Fig. 9). These data were well approximated in the least-squared sense by a linear function (upper-level FREE: $R^2 = 0.60$, $p = 0.009$; lower-level FREE: $R^2 = 0.50$, $p = 0.023$; upper-level FIXED: $R^2 = 0.52$, $p = 0.019$; lower-level FIXED: $R^2 = 0.61$, $p = 0.008$).

4. Discussion

In this study, we quantified the referent aperture (R_a) and the synergistic organization of mechanical and control variables involved in the static grasp of a fixed and a free object. The data supported the four hypotheses formulated in the *Introduction*. We found that the apparent digit stiffness (k) and width of the R_a were larger in free- than in fixed-object prehension (hypothesis H1). We also confirmed that the midpoint of R_a was skewed toward the virtual finger (hypothesis H2). Further, synergic organization for the stabilization of total force on the object was observed in the space of the control variables {*RC*, *k*} as well as in the space of the digit forces (hypothesis H3). Lastly, we observed relatively large strength of synergies at the higher level of the hierarchy in the free condition than in fixed condition (hypothesis H4). These results add to the current literature by demonstrating that grasp control involves modulation of digit apparent stiffness in addition to the referent coordinate and by identifying the synergistic organization of the control variables during static grasp.

4.1. Effect of mechanical constraints on the formation of the referent aperture for grip force production

Comparing the hypothetical control variables {*RC*, *k*} across the two tasks – the static grasp of the free and the fixed handle – allowed us to identify the functional roles of the variables in managing grasp stability. We note that the *RC* and *k* are measurable surrogates for two neural control signals (Ambike, Mattos, Zatsiorsky, & Latash, 2018) that form a hierarchy (Feldman, 2015). Specifically, the R-command defines the spatial coordinate (*RC*), and the C-command (associated with *k*) is associated with a co-activation zone about the spatial coordinate defined by the R-command. The R-command influences the position and/or the contact forces, and the C-command is associated with the stiffness of the effector. Therefore, the changes in *RC* and *k* can be interpreted as arising from the underlying R- and C-commands.

The passive mechanical stiffness (i.e., with no spinal reflexes) of the virtual finger is over twice that of the thumb (1.17 N/mm vs 0.46 N/mm) (Park, Pazin, Friedman, Zatsiorsky, & Latash, 2014). While grasping, however, this passive stiffnesses will be modulated via the tonic stretch reflex, thus yielding the apparent stiffness, and the apparent stiffness increases with the magnitude of the generated digit force (Feldman & Orlovsky, 1972). Therefore, we controlled the digit force across grasping conditions. Indeed, the

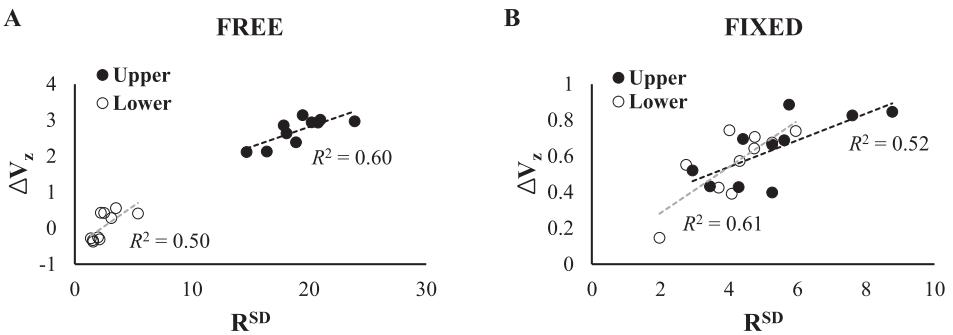

Fig. 9. Relationship between R^{SD} and ΔV_Z in the (A) FREE and (B) FIXED condition. Linear regression was performed separately for each hierarchy using data pooled across subjects. Black circle and open circle represent upper and lower-level, respectively. The best-fit regression line with R^2 values are presented for each hierarchy.

thumb and the virtual finger forces between the two conditions w ere not significantly different (Fig. 4A).

Despite the consistent force, k was higher for the TH and VF in the FREE compared to the FIXED condition (Fig. 4C). Correspondingly, the aperture width (R_a^w) was smaller by 73% (about 12 mm) for the FREE condition. One interpretation of this finding is that the muscle co-activation (C-command) of the hand/finger system was larger in the free object prehension, likely to maintain the stability of the grasp. In contrast, when the stability of the handle was ensured by the surrounding support structure, the human control system responded by reducing the digit stiffnesses and using a smaller referent aperture instead. Thus, a possible strategy to set the two control variables is the increment of k, and a decrement of RC; this may be a way to prevent the slip and enlarge safety margin (Singh & Ambike, 2017) without changes in the force magnitude.

The midpoint of R_a (R_a^m) was located within approximately 3–4 mm of the center of the handle along the horizontal axis (i.e., z-axis) regardless of whether the handle was externally constrained or not. In particular, R_a^m was closer to the virtual finger (Fig. 5), which was associated with the larger apparent stiffness (k). Note that the difference in the apparent stiffnesses of the thumb and the virtual finger during grasping mirrored the difference in their passive stiffnesses (Park et al., 2014). This may be explained in part by the fact that the virtual finger is comprised of four fingers, and its apparent stiffness is the addition of four spring stiffnesses, one per finger, arranged in parallel. It is unclear whether this TH-VF asymmetry in terms of the RC and k (and the corresponding shift in R_a^m) is functional, or whether it is a characteristic arising from the structure of the human hand (4 fingers in opposition with one thumb). This point needs to be clarified in the future studies.

However, our results of the two control variables in the free object prehension task point to the functional roles of individual fingers. Notably, there were no significant differences in the magnitudes of individual finger forces in the FREE condition (Fig. 4A), while {RC, k} showed significant main effect of *Finger* (Fig. 4B, C). Previous studies showed that the central fingers, M and R, are responsible primarily for resultant force production, whereas the lateral fingers, I and L, are specialized for rotational action, i.e., moment of force production (Zatsiorsky & Latash, 2008). This interpretation was further supported by the coefficients of the quadratic objective function that explained the across-finger force distribution when the four fingers produce pressing forces (Park, Singh, Zatsiorsky, & Latash, 2012). Here, we observed larger k value for the lateral index finger, which may be helpful to maintain the rotational equilibrium.

A recent study suggested a more complete set of referent variables for describing the grasp of a free object in a gravity field and in the presence of external torques (Ambike et al., 2014; Latash et al., 2010). There was not only R_a, but also a *referent orientation (angle)* and *referent vertical coordinate* reflecting the rotational equilibrium constraint and load forces, respectively. We observed that the k of the index finger was greater than the other fingers in both prehension conditions (Fig. 4C). This difference in k between fingers was consistent with the previous finding (Park et al., 2014). A large k value implies a more rapid change in the corresponding digit normal force when the handle is expanded, and this change results in a manipulation moment that can change the orientation of the handle. In the current study, the high k of the index finger changed the direction of the moment of normal force during the handle expansion phase, but the resultant moment was kept constant and the change in handle orientation was minimized due to the compensatory behavior of the moment of tangential force. Note that the "do not intervene" paradigm employed in our experiment did not dictate either the digit forces or orientation of the handle. Therefore, the fact that the produced moment during aperture expansion caused by the unbalanced k among four fingers while not reacting to the handle expansion was naturally canceled by another moment component, partially supports the existence of the referent orientation as an independent control variable to produce a required net moment on the object. This result is similar to the *principle of superposition* which states that the control for translational and rotational stability could be decoupled in the grasping task (Shim, Latash, & Zatsiorsky, 2005b; Shim & Park, 2007).

Although we measured both normal and tangential forces during multi-digit prehension, our analyses were restricted to the horizontal axis. Grasp stability would be influenced by normal and tangential forces, and any interaction between these forces would influence our interpretations. However, the PCA showed that the normal and tangential digit forces were decoupled (indicated by the loading factors for the first 2 PCs; Table 1). The decoupling implies that the fine tuning (i.e., synergic action) of two groups of forces is organized independently. Therefore, the estimation and interpretation of the control variables along the direction of the normal forces without the consideration of tangential forces is reasonable. Nevertheless, we admit that the current study could estimate only R_a because our device changed the position of the digits along the direction of normal forces only. Quantification of other referent variables (i.e., referent angle and referent vertical coordinate) is required, and we aim to accomplish this reconstruction in our future study.

4.2. Hierarchical organization of control variables for grip stability

We observed synergies for the stabilization of the net grasping force (F_{TOT}^N) around zero in the space of the thumb and virtual finger forces as well as the space of {RC, k}. In addition, stronger synergies were observed when the digits were responsible for ensuring adherence to the mechanical constraints of static prehension, i.e., in the FREE condition. The two types of synergies – one between the digit forces (obtained via the UCM analysis) and one between the control variables (obtained with the permutation analysis) provide consistent results, as shown by the positive correlations in Fig. 9; thus, the permutation analysis of {RC, k} can be used to assess the stability of the grasp.

Recent studies based on the theory of referent configuration provide ample evidence that the referent configuration is possibly a control variable at a higher level of a control hierarchy. In other words, the reference configuration defines a set of thresholds values of all involved muscles for the given task (i.e., the threshold of the tonic stretch reflex). In the present case, the referent variables {RC, k} at the Hand level (Fig. 1B) are the salient performance variables that are specified at the higher level of the hierarchy, which yield grasp force and stability as a consequence of the interactions between the body effectors and the object. A series of few-to-many

transformations yield variables at the lower levels of the control hierarchy. This idea, which originated from the equilibrium-point hypothesis (Feldman, 1986), is compatible with the concept of the hierarchy of motor synergies (Gorniak et al., 2009); hierarchical organization of motor synergies has been observed in finger force or force-mode spaces (Latash, Scholz, & Schoner, 2007). That is, the controller governs only task level variables of motor actions, and the features such as the activation and covariation of individual finger forces seem to be a secondary consideration within the scope of control by the CNS. Indeed, the pattern of covariation between the variables at a higher level does not specify the unique combination of the lower-level variables in a redundant biological system (Latash, 2020a). Previous theoretical studies (Cutkosky & Howe, 1990; Iberall, 1997) and experimental studies on hand and finger actions (Baud-Bovy & Soechting, 2001; Santello & Soechting, 1997; Shim et al., 2003) have suggested a hierarchical control of multi-digit prehension based on the notions of the virtual finger (VF) and individual finger (IF), i.e., at the higher level (VF level) the thumb and VF are coordinated to satisfy task mechanics whereas at the lower level (IF level) the individual fingers are coordinated to generate a desired task-specific outcome of the virtual finger. In other words, the higher-level variables are coordinated to stabilize salient performance variables, whereas at the lower-level are coordinated to generate a desired task-specific outcome that has a mechanical link to the higher-level variables. Indeed, it has been reported that the net normal forces were stabilized only at the task level during multi-finger pressing and prehensile tasks with the thumb and fingers (Gorniak et al., 2009; Kang, Shinohara, Zatsiorsky, & Latash, 2004; Park et al., 2015; Shim et al., 2003).

Our results here are in line with the previous findings. We observed synergies in both the spaces of force and control variable in the upper level of the hierarchy for the Free condition, but the synergies vanished at the lower level (Figs. 6, 8A, 9A). This indicates that the covariation between the fingers functioned to *destabilize* the VF normal force; this may assist the VF to respond to changes in the thumb normal force so that the total force on the handle is stabilized (Gorniak et al., 2009). Further, when the constraints on the digit behavior were removed by externally fixing the object, the synergies in both spaces at the upper hierarchical level declined (Figs. 6A, 8A). However, the synergy indices were still greater than the corresponding critical values, indicating that the subjects were able to coordinate the thumb and VF forces and $\{RC, k\}$ values to maintain close to zero value of total normal force. In contrast, the synergy indices at the lower hierarchical level were higher for the Fixed relative to the Free condition. The magnitudes of these synergy indices were low, however, and this effect may be a biproduct of the changes in synergistic organization at the upper level. Since the VF normal force does not need to change in response to the thumb normal force, the fingers are not as coordinated to destabilize the VF normal force.

5. Conclusion

This study quantified the referent aperture location and width – the postulated control variables within the referent control theory – for the control of multi-finger grasping by reconstructing the digit referent positions (*RC*s) and apparent stiffnesses (k). We found large k and referent aperture when holding a free object compared to holding an object that is externally constrained; the larger digit stiffness is important when the digits are responsible for grip stability. The referent aperture was located closer to the virtual finger than the thumb, and it was not the centered within the actual aperture. More work is required to identify whether this asymmetry has functional origins, or whether it is a characteristic of the structure of the grasp, with four fingers in opposition with one thumb. We also demonstrated the stabilization of critical task variables via synergistic covariation in the control variables *RC* and k as well as in the digit forces at two different levels of the control hierarchy. Furthermore, we demonstrated that the synergistic organization of the variables is sensitive to the presence/absence of external constraints on the object. The relatively small sample size makes the current conclusion tentative, albeit the current results had subtle statistical power. Thus, it needs to be replicated in a larger cohort to robust the current conclusion. Overall, our findings extend the ideas on grasp control with referent configurations by demonstrating that the digit apparent stiffness is modulated in addition to the digit referent coordinate for grip control, and by quantifying the synergistic organization of various control variables in the control hierarchy.

Funding

This research was in part supported by the Basic Research Program through the National Research Foundation of Korea (NRF) funded by the MSIT (2022R1A4A503404611) and the Basic Science Research Program through the National Research Foundation of Korea (NRF) funded by the Ministry of Education (2021R1I1A4A01041781).

CRediT authorship contribution statement

Junkyung Song: Conceptualization, Methodology, Investigation, Data curation, Formal analysis, Writing – original draft, Writing – review & editing. **Kitae Kim:** Methodology, Investigation, Visualization, Writing – original draft. **Satyajit Ambike:** Conceptualization, Methodology, Validation, Writing – review & editing. **Jaebum Park:** Supervision, Project administration, Conceptualization, Validation, Writing – original draft, Writing – review & editing.

Declaration of Competing Interest

There are no conflicts of interest to declare.

References

Ambike, S., Mattos, D., Zatsiorsky, V., & Latash, M. (2018). Systematic, unintended drifts in the cyclic force produced with the fingertips. *Motor Control, 22*(1), 82–99. https://doi.org/10.1123/mc.2016-0082

Ambike, S., Mattos, D., Zatsiorsky, V. M., & Latash, M. L. (2016). Synergies in the space of control variables within the equilibrium-point hypothesis. *Neuroscience, 315*, 150–161. https://doi.org/10.1016/j.neuroscience.2015.12.012

Ambike, S., Paclet, F., Zatsiorsky, V. M., & Latash, M. L. (2014). Factors affecting grip force: Anatomy, mechanics, and referent configurations. *Experimental Brain Research, 232*(4), 1219–1231. https://doi.org/10.1007/s00221-014-3838-8

Ambike, S., Zhou, T., Zatsiorsky, V. M., & Latash, M. L. (2015). Moving a hand-held object: Reconstruction of referent coordinate and apparent stiffness trajectories. *Neuroscience, 298*, 336–356. https://doi.org/10.1016/j.neuroscience.2015.04.023

Arbib, M. A., Iberall, T., & Lyons, D. (1985). Coordinated control programs for movements of the hand. *Experimental Brain Research*, 111–129.

Baud-Bovy, G., & Soechting, J. F. (2001). Two virtual fingers in the control of the tripod grasp. *Journal of Neurophysiology, 86*(2), 604–615. https://doi.org/10.1152/jn.2001.86.2.604

Cuadra, C., Wojnicz, W., Kozinc, Z., & Latash, M. L. (2020). Perceptual and motor effects of muscle co-activation in a force production task. *Neuroscience, 437*, 34–44. https://doi.org/10.1016/j.neuroscience.2020.04.023

Cutkosky, M. R., & Howe, R. D. (1990). Human grasp choice and robotic grasp analysis. In S. T. Venkataraman, & T. Iberall (Eds.), *Dextrous robot hands* (pp. 5–31). NY: Springer.

Feldman, A. G. (1966). Functional tuning of nervous system during control of movement or maintenance of a steady posture. 3. Mechanographic analysis of execution by man of simplest motor tasks. *Biophysics USSR, 11*(4), 766.

Feldman, A. G. (1986). Once more on the equilibrium-point hypothesis (lambda-model) for motor control. *Journal of Motor Behavior, 18*(1), 17–54.

Feldman, A. G. (2015). *Referent control of action and perception: Challenging conventional theories in behavioral neuroscience*. NY: Springer.

Feldman, A. G., & Orlovsky, G. N. (1972). The influence of different descending systems on the tonic stretch reflex in the cat. *Experimental Neurology, 37*(3), 481–494.

Frenkel-Toledo, S., Yamanaka, J., Friedman, J., Feldman, A. G., & Levin, M. F. (2019). Referent control of anticipatory grip force during reaching in stroke: An experimental and modeling study. *Experimental Brain Research, 237*(7), 1655–1672. https://doi.org/10.1007/s00221-019-05498-y

Gao, F., Latash, M., & Zatsiorsky, V. (2004). Neural network modeling supports a theory on the hierarchical control of prehension. *Neural Computing & Applications, 13*(4), 352–359. https://doi.org/10.1007/s00521-004-0430-3

Gorniak, S. L., Zatsiorsky, V. M., & Latash, M. L. (2009). Hierarchical control of static prehension: II. Multi-digit synergies. *Experimental Brain Research, 194*(1), 1–15. https://doi.org/10.1007/s00221-008-1663-7

Iberall, T. (1997). Human prehension and dexterous robot hands. *International Journal of Robotics Research, 16*(3), 285–299. https://doi.org/10.1177/027836499701600302

Kaiser, H. F. (1960). The application of electronic-computers to factor-analysis. *Educational and Psychological Measurement, 20*(1), 141–151. https://doi.org/10.1177/001316446002000116

Kang, N., Shinohara, M., Zatsiorsky, V. M., & Latash, M. L. (2004). Learning multi-finger synergies: An uncontrolled manifold analysis. *Experimental Brain Research, 157*(3), 336–350. https://doi.org/10.1007/s00221-004-1850-0

Latash, M. L. (1994). Reconstruction of equilibrium trajectories and joint stiffness patterns during single-joint voluntary movements under different instructions. *Biological Cybernetics, 71*(5), 441–450. https://doi.org/10.1007/Bf00198920

Latash, M. L. (2010). Motor synergies and the equilibrium-point hypothesis. *Motor Control, 14*(3), 294–322.

Latash, M. L. (2018). Muscle coactivation: Definitions, mechanisms, and functions. *Journal of Neurophysiology, 120*(1), 88–104. https://doi.org/10.1152/jn.00084.2018

Latash, M. L. (2020a). Laws of nature that define biological action and perception. *Physics of Life Reviews, 36*, 47–67. https://doi.org/10.1016/j.plrev.2020.07.007

Latash, M. L. (2020b). On primitives in motor control. *Motor Control, 24*(2), 318–346. https://doi.org/10.1123/mc.2019-0099

Latash, M. L., Friedman, J., Kim, S. W., Feldman, A. G., & Zatsiorsky, V. M. (2010). Prehension synergies and control with referent hand configurations. *Experimental Brain Research, 202*(1), 213–229. https://doi.org/10.1007/s00221-009-2128-3

Latash, M. L., Scholz, J. P., & Schoner, G. (2007). Toward a new theory of motor synergies. *Motor Control, 11*(3), 276–308. https://doi.org/10.1123/mcj.11.3.276

MacKenzie, C. L., & Iberall, T. (1994). *The grasping hand*. Elsevier.

Muller, H., & Sternad, D. (2003). A randomization method for the calculation of covariation in multiple nonlinear relations: Illustrated with the example of goal-directed movements. *Biological Cybernetics, 89*(1), 22–33. https://doi.org/10.1007/s00422-003-0399-5

Oldfield, R. C. (1971). The assessment and analysis of handedness: The Edinburgh inventory. *Neuropsychologia, 9*(1), 97–113. https://doi.org/10.1016/0028-3932(71)90067-4

Park, J., Baum, B. S., Kim, Y. S., Kim, Y. H., & Shim, J. K. (2012). Prehension synergy: Use of mechanical advantage during multifinger torque production on mechanically fixed and free objects. *Journal of Applied Biomechanics, 28*(3), 284–290. https://doi.org/10.1123/jab.28.3.284

Park, J., Han, D. W., & Shim, J. K. (2015). Effect of resistance training of the wrist joint muscles on multi-digit coordination. *Perceptual and Motor Skills, 120*(3), 816–840. https://doi.org/10.2466/25.26.PMS.120v16x9

Park, J., Kim, Y. S., & Shim, J. K. (2010). Prehension synergy: Effects of static constraints on multi-finger prehension. *Human Movement Science, 29*(1), 19–34. https://doi.org/10.1016/j.humov.2009.11.001

Park, J., Lewis, M. M., Huang, X. M., & Latash, M. L. (2013). Effects of olivo-ponto-cerebellar atrophy (OPCA) on finger interaction and coordination. *Clinical Neurophysiology, 124*(5), 991–998. https://doi.org/10.1016/j.clinph.2012.10.021

Park, J., Pazin, N., Friedman, J., Zatsiorsky, V. M., & Latash, M. L. (2014). Mechanical properties of the human hand digits: Age-related differences. *Clinical Biomechanics, 29*(2), 129–137. https://doi.org/10.1016/j.clinbiomech.2013.11.022

Park, J., Singh, T., Zatsiorsky, V. M., & Latash, M. L. (2012). Optimality versus variability: Effect of fatigue in multi-finger redundant tasks. *Experimental Brain Research, 216*(4), 591–607. https://doi.org/10.1007/s00221-011-2963-x

Pilon, J. F., De Serres, S. J., & Feldman, A. G. (2007). Threshold position control of arm movement with anticipatory increase in grip force. *Experimental Brain Research, 181*(1), 49–67. https://doi.org/10.1007/s00221-007-0901-8

Reschechtko, S., & Latash, M. L. (2017). Stability of hand force production. I. Hand level control variables and multifinger synergies. *Journal of Neurophysiology, 118*(6), 3152–3164. https://doi.org/10.1152/jn.00485.2017

Reschechtko, S., & Latash, M. L. (2018). Stability of hand force production. II. Ascending and descending synergies. *Journal of Neurophysiology, 120*(3), 1045–1060. https://doi.org/10.1152/jn.00045.2018

Santello, M., & Soechting, J. F. (1997). Matching object size by controlling finger span and hand shape. *Somatosensory and Motor Research, 14*(3), 203–212.

Savescu, A. V., Latash, M. L., & Zatsiorsky, V. M. (2008). A technique to determine friction at the fingertips. *Journal of Applied Biomechanics, 24*(1), 43–50. https://doi.org/10.1123/jab.24.1.43

Shim, J. K., Latash, M. L., & Zatsiorsky, V. M. (2003). Prehension synergies: Trial-to-trial variability and hierarchical organization of stable performance. *Experimental Brain Research, 152*(2), 173–184. https://doi.org/10.1007/s00221-003-1527-0

Shim, J. K., Latash, M. L., & Zatsiorsky, V. M. (2005a). Prehension synergies in three dimensions. *Journal of Neurophysiology, 93*(2), 766–776. https://doi.org/10.1152/jn.00764.2004

Shim, J. K., Latash, M. L., & Zatsiorsky, V. M. (2005b). Prehension synergies: Trial-to-trial variability and principle of superposition during static prehension in three dimensions. *Journal of Neurophysiology, 93*(6), 3649–3658. https://doi.org/10.1152/jn.01262.2004

Shim, J. K., & Park, J. B. (2007). Prehension synergies: Principle of superposition and hierarchical organization in circular object prehension. *Experimental Brain Research, 180*(3), 541–556. https://doi.org/10.1007/s00221-007-0872-9

Singh, T., & Ambike, S. (2017). A soft-contact model for computing safety margins in human prehension. *Human Movement Science, 55*, 307–314. https://doi.org/10.1016/j.humov.2017.03.006

Wu, Y. H., Zatsiorsky, V. M., & Latash, M. L. (2012). Static prehension of a horizontally oriented object in three dimensions. *Experimental Brain Research, 216*(2), 249–261. https://doi.org/10.1007/s00221-011-2923-5

Zatsiorsky, V. M., Gao, F., & Latash, M. L. (2006). Prehension stability: Experiments with expanding and contracting handle. *Journal of Neurophysiology, 95*(4), 2513–2529. https://doi.org/10.1152/jn.00839.2005

Zatsiorsky, V. M., Gregory, R. W., & Latash, M. L. (2002a). Force and torque production in static multifinger prehension: Biomechanics and control. I. Biomechanics. *Biological Cybernetics, 87*(1), 50–57. https://doi.org/10.1007/s00422-002-0321-6

Zatsiorsky, V. M., Gregory, R. W., & Latash, M. L. (2002b). Force and torque production in static multifinger prehension: Biomechanics and control. II. Control. *Biological Cybernetics, 87*(1), 40–49. https://doi.org/10.1007/s00422-002-0320-7

Zatsiorsky, V. M., & Latash, M. L. (2008). Multifinger prehension: An overview. *Journal of Motor Behavior, 40*(5), 446–475. https://doi.org/10.3200/Jmbr.40.5.446-476